Thermal Response of Narrow-Disperse Poly(*N*-isopropylacrylamide) Prepared by Atom Transfer Radical Polymerization

Yan Xia, Xiangchun Yin, Nicholas A. D. Burke, and Harald D. H. Stöver*

Department of Chemistry, McMaster University, Hamilton, Ontario, Canada L8S 4M1

Received February 4, 2005; Revised Manuscript Received May 6, 2005

ABSTRACT: Room temperature atom transfer radical polymerizations of *N*-isopropylacrylamide (NIPAM) carried out in 2-propanol (*i*-PrOH) and *tert*-butyl alcohol (*t*-BuOH) resulted in PNIPAMs with polydispersities between 1.1 and 1.2 and degrees of polymerization of up to 300. Methyl 2-chloropropionate (MCP), copper(I) chloride, and tris[2-(dimethylamino)ethyl]amine (Me_6TREN) were used as initiator, catalyst, and ligand in a 1:1:1 ratio. Conversions were as high as 91 and 79%, respectively, without the need for excess catalyst as was required in previous studies. Aqueous solutions of these narrow-disperse PNIPAMs showed a strong decrease of the phase transition temperature with increasing molecular weight, as measured by turbidimetry and differential scanning calorimetry. In low molecular weight samples, containing significant oligomeric fractions, the slightly hydrophobic methyl propionate end group becomes significant and further decreases the onset temperature of the phase transition.

Introduction

Polymers such as poly(*N*-isopropylacrylamide) (PNIPAM) and its copolymers that can respond to external stimuli are of great interest for the design of "intelligent" materials.[1−4] Aqueous solutions of PNIPAM exhibit a reversible liquid−solid phase transition with a lower critical solution temperature (LCST) around 32 °C. This LCST phenomenon is attributed to the entropy increase from the loss of hydrophobic interactions between the isopropyl groups of the polymer and water upon heating.[1,2,5−7]

While there have been extensive studies regarding the effects of polymer concentration,[1,8] cosolvent,[9,10] pressure,[11] and the presence of salts[7] or surfactants,[12,13] the effect of molecular weight on the LCST of PNIPAM is not yet clear. The LCSTs of NIPAM homopolymers have been reported to be inversely dependent,[6] directly dependent,[8] or independent[5,14,15] of the molecular weight. A similar situation exists for other thermoresponsive polymers including other polyacrylamides.[16−22] While the use of different radical initiators and hence end groups, different polymer concentrations, and different techniques for measuring LCSTs accounts for some of these variations, previous studies also relied on partially fractionated[5,8,14,15] or unfractionated[6] PNIPAM samples obtained from conventional radical polymerizations, which often had broad polydispersities. These polydisperse samples may have precluded precise examination of molecular weight effect on LCST because the low or high molecular weight fraction, whichever has a lower LCST, may mask the LCST of the bulk of the sample. A definitive answer hence would require the synthesis of PNIPAMs with well-controlled molecular weights and end groups.

The preparation of linear narrow-disperse PNIPAM by reversible addition−fragmentation transfer (RAFT) polymerization[23] was recently reported,[24−27] and nitroxide-mediated radical polymerization (NMP)[28] was used to graft PNIPAM from a polystyrene star macroinitiator.[29] Atom transfer radical polymerization (ATRP)[30] is especially attractive as it can provide good control over both polymer molecular weight and end groups; however, the ATRP of acrylamides including NIPAM has remained challenging. The groups of Matyjaszewski and Brittain reported that ATRP of *N*,*N*-dimethylacrylamide (DMA) suffered from (a) deactivation of the copper catalyst through complexation with amide groups, (b) displacement of the terminal halide atom by amide groups, and (c) low values of the ATRP equilibrium constant.[31,32] Using alkyl chlorides rather than bromides as initiators in conjunction with tris[2-(dimethylamino)-ethyl]amine (Me_6TREN) as ligand improved the control, though high conversions typically required high catalyst-to-initiator ratios (2:1 or 3:1).[33,34] Recently, Masci et al. reported the successful ATRP of NIPAM in dimethylformamide/water mixtures; however, degrees of polymerization (DP) of 200 still required higher catalyst/initiator ratios, likely again due to extensive catalyst deactivation.[35]

Scheme 1

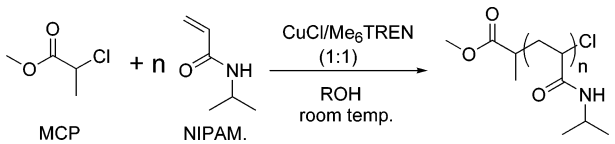

Our group recently studied linear[36−40] and cross-linked[38,39] thermoresponsive polymers, including copolymers of DMA with hydrophobic comonomers suitable for subsequent cross-linking such as glycidyl methacrylate and allyl methacrylate.[38,39] As part of that work, we prepared DMA/*N*-phenylacrylamide copolymers with narrow molecular weight distributions using atom transfer radical polymerization (ATRP) in methanol and methanol/water mixtures.[40]

In this paper, we describe the synthesis of PNIPAM by ATRP in alcohols, using methyl 2-chloropropionate (MCP)/CuCl/Me_6TREN (1:1:1) as the initiating system (Scheme 1). We then describe for the first time the molecular weight dependence of the cloud points of aqueous solutions of narrow-disperse PNIPAM.

* Corresponding author. E-mail stoverh@mcmaster.ca.

10.1021/ma050261z CCC: $30.25
Published on Web 06/15/2005

Experimental Section

N-Isopropylacrylamide (Aldrich, 97%) was recrystallized twice from benzene/hexane prior to use. Copper(I) chloride (97%), copper(II) chloride (99.99%), methyl 2-chloropropionate (97%), and tetrabutylammonium bromide (99%) were purchased from Aldrich and used as received. Me_6TREN was prepared as described in the literature.[41] Methanol (MeOH, Caledon, HPLC grade), ethanol (EtOH, Commercial Alcohols), 1-propanol (*n*-PrOH, Fisher, Certified), 2-propanol (*i*-PrOH, Fisher, HPLC grade), *tert*-butyl alcohol (*t*-BuOH, Fisher, Certified), tetrahydrofuran (THF, Caledon, HPLC grade), and pentane (Caledon, >98%) were used as received. Azobis(isobutyronitrile) was obtained as a gift from Dupont.

General Procedure for ATRP of NIPAM. To prepare PNIPAM with target degree of polymerization of 50, NIPAM (2.00 g, 17.7 mmol), CuCl (0.035 g, 0.35 mmol), and 2-propanol (4.00 g), deoxygenated by bubbling with nitrogen for at least 30 min, were combined and then transferred to a nitrogen-purged 25 mL round-bottom flask fitted with a septum. Me_6-TREN (0.081 g, 0.35 mmol) was added via a nitrogen-purged syringe, and the solution was stirred for 20 min to allow formation of the CuCl/Me_6TREN complex. MCP (0.043 g, 0.35 mmol) was then added using a syringe to begin the polymerization. The reactions were carried out at room temperature under a slight positive pressure of nitrogen.

Aliquots (0.6 mL) were removed at regular intervals, divided between two vials in a 5:1 ratio, and dried under a stream of air. The smaller sample was dissolved in THF, passed through a short silica column to remove the catalyst, dried under a stream of air, and used for gel permeation chromatography (GPC) analysis. The larger portion of the aliquot was used to determine conversion in one of two ways. For polymerizations in MeOH or *t*-BuOH, conversion was measured directly with ^{1}H NMR spectroscopy in D_2O by comparison of the peak areas of monomer signals at 5.7 ppm (one proton) or 6.2 ppm (two protons) with the polymer signal at 3.9 ppm (one proton) corrected for contribution due to monomer. For reactions in EtOH, *n*-PrOH, or *i*-PrOH, the dried sample was first reprecipitated from THF into pentane (1:12 v/v) and dried to constant weight under vacuum at 60 °C. Conversion was then determined gravimetrically and corrected for residual monomer using ^{1}H NMR spectroscopy.

Conventional Free Radical Polymerization of NIPAM. NIPAM (0.5 g, 4.4 mmol), AIBN (7.3 mg, 0.044 mmol), and methyl ethyl ketone (7 mL) were placed in a 25 mL screw-cap glass vial. The vial was heated for 11.5 h at 65 °C in an oven while being rotated at 18 rpm. The polymer was isolated by precipitation in pentane, purified by precipitation from THF into pentane four times, and then dried to constant weight in a vacuum oven to afford 0.27 g (54% yield) of PNIPAM as a white powder. $M_{n,GPC}$ = 28.9 kDa, PDI = 2.00.

Polymer Characterization. Average molecular weights and molecular weight distributions were determined by GPC on a Waters GPC system consisting of a Waters 515 HPLC pump, a Waters 717plus Autosampler, three Waters Styragel columns (HR2, HR3, and HR4; 30 cm × 7.8 mm; 5 μm particles; exclusion limits: 500−20000, 500−30000, and 5000−600000 g/mol, respectively) maintained at 40 °C, and a Waters 2414 refractive index detector maintained at 35 °C. THF containing 0.25% (w/v) tetrabutylammonium bromide was used as the mobile phase (0.8 mL/min), and the system was calibrated with narrow-disperse polystyrene standards.

^{1}H NMR spectra were measured on Bruker AV 200 or DRX 500 spectrometers with samples dissolved in D_2O.

Samples for matrix-assisted laser desorption ionization-time-of-flight (MALDI−TOF) analysis were prepared by combining THF solutions of dithranol (20 mg/mL), PNIPAM (10 mg/mL), and sodium acetate (10 mg/mL) in a 10:1:1 ratio. MALDI−TOF spectra were acquired with a Micromass TofSpec 2E (20 kV operating voltage, 337 nm N_2 laser) in linear or reflectron mode. MALDI-QTOF spectra were collected on a Micromass Global Ultima (9.1 kV operating voltage, 337 nm N_2 laser, MALDI mode) in reflectron mode.

Cloud points were measured on a Cary 100 Bio UV−vis spectrophotometer equipped with a temperature-controlled, six-position sample holder. Aqueous PNIPAM solutions (1 wt %) were heated at 0.2 °C/min while both the transmittance at 500 nm (1 cm path length) and the solution temperature, as determined by the internal temperature probe, were monitored.

A TA Instruments DSC 2910 differential scanning calorimeter (DSC) was used to measure the phase transition temperature of 1 wt % PNIPAM solutions (≈30 μL) in hermetic aluminum crimp-seal pans while scanning at 1 °C/min. The temperatures of both the onset and maximum of the endotherm were determined. The DSC was calibrated with an indium standard for temperature and enthalpy changes.

Results and Discussion

Solvent Effect on ATR Polymerization of NIPAM. Alcohols were chosen as the solvents for ATRP on the basis of the premise that a hydrogen-bonding solvent could bind to the amide groups of both monomer and polymer and thus reduce their interaction with both catalyst and propagating chain end. A similar approach had been used successfully in the ATRP of other strongly coordinating monomers, DMA[40] and 4-vinylpyridine.[42] Alcohols can dissolve many monomer/polymer and catalyst systems and range widely in their hydrogen-bonding ability and polarity, permitting optimization of the polymerization. In this work, we explored ATRP of NIPAM in five alcohols: methanol, ethanol, 1-propanol, 2-propanol, and *tert*-butyl alcohol.

Monomer conversion and polymer molecular weight were determined at different stages during each polymerization. Conversions for polymerizations carried out in MeOH and *t*-BuOH were measured by ^{1}H NMR spectroscopy, while others were determined gravimetrically. Polymer molecular weights (MWs) and polydispersity indices (PDIs) were determined by a GPC method as developed by Müller.[25] This method had been established to give reproducible results, though with MW values significantly higher than those obtained from MALDI−TOF analysis,[25] and, therefore, the MW values determined by GPC in our work were only used to reveal trends. More precise molecular weights were determined using ^{1}H NMR spectroscopy by comparing the peak areas of the polymer isopropyl C−H signal at 3.9 ppm, with the methoxy signal at 3.8 ppm arising from the MCP initiator. The M_n values determined by either GPC ($M_{n,GPC}$) or NMR ($M_{n,NMR}$) increased in proportion to the monomer:initiator (M:I) ratio (Table 1), and $M_{n,NMR}$ values were in reasonably good agreement with theoretical values.

The results for ATRP of NIPAM in the five alcohols are summarized in Table 1 and Figure 1 and show increasing monomer conversion along the series of alcohols MeOH, EtOH, *n*-PrOH, *i*-PrOH, and *t*-BuOH. Polymerizations in methanol turned deep blue as soon as the initiator was added, indicating high Cu(II) concentrations. This polymerization reached a plateau in conversion after 2 h (Figure 1).

ATRP in EtOH and *n*-PrOH provided higher conversions, reaching ∼65% after 6 h, but the first-order kinetic plots (Figure 2) show significant curvature. However, the low polydispersity index (PDI) at the end of polymerization shows that the growing centers were not lost, as this would have led to a much broader MW distribution. Therefore, the apparent curvature of the first-order kinetic plots is attributed to a progressive reduction of the concentration of the available catalyst. Analogous behavior has been observed for this initiating

Table 1. Monomer Conversion, Molar Mass (M_n), and Polydispersity (M_w/M_n) Data for Atom Transfer Radical Polymerization (ATRP) of *N*-Isopropylacrylamide (NIPAM) in Alcohols[a]

solvent	$[M]_0$:$[I]_0$ (M/solvent) (w/w)	time (h)	conv (%)	$M_{n,th}$[b]	$M_{n,GPC}$[c]	$M_{n,NMR}$[d]	M_w/M_n[c]
MeOH	100:1 (1/2)	7	32	3600	3800		1.13
EtOH	100:1 (1/2)	9.5	64	7200	10 400		1.09
n-PrOH	100:1 (1/2)	6	66	7500	12000		1.07
i-PrOH	50:1 (1/2)	4	89	5000	8000	5000	1.15
i-PrOH	100:1 (1/2)	7	91	10 300	17 300	8400	1.13
i-PrOH	200:1 (1/2)	8	79	17 900	35 600	15 700	1.13
i-PrOH	200:1 (1/1)	4.5	78	17 600	44 200	16 400	1.14
i-PrOH	400:1 (1/2)	12	73	33 000	67 600	27 300	1.27
i-PrOH	400:1 (1/1)	5.6	72	32 500	67 600	26 500	1.16
t-BuOH	50:1 (1/2)	3	79	4500	7300	4400	1.15
t-BuOH	100:1 (1/2)	4	76	8600	14300	6700	1.16
t-BuOH	200:1 (1/2)	4	76	17 200	37 500	14 400	1.14

[a] Experimental conditions: typically 3 g of NIPAM; MCP:CuCl:Me_6TREN = 1:1:1; room temperature. [b] $M_{n,th} = M_{NIPAM}[NIPAM]_0 conv/[MCP]_0$. [c] From GPC in 0.25% (w/v) Bu_4NBr/THF. [d] From ^1H NMR spectroscopy (500 MHz) in D_2O, 25 or 30 °C.

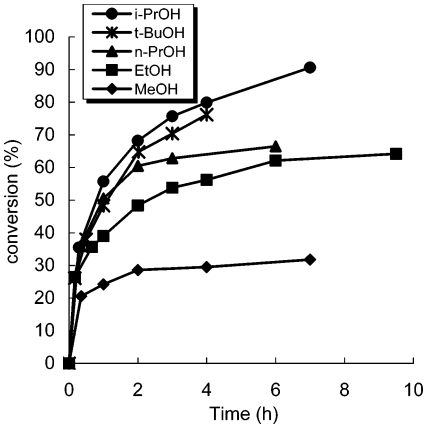

Figure 1. Monomer conversion vs time curves for ATRP of NIPAM in different alcohols. Conditions: NIPAM:MCP:CuCl:Me_6TREN = 100:1:1:1; NIPAM:solvent = 1:2 (w/w); room temperature.

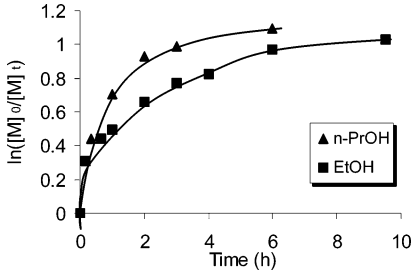

Figure 2. Kinetic plot for the ATRP of NIPAM in EtOH and *n*-PrOH. Conditions: NIPAM/ROH = 1/2 (w/w); NIPAM:MCP:CuCl:Me_6TREN = 100:1:1:1; room temperature.

system during the ATRP of DMA in toluene.[33,34] Hence, while MCP/CuCl/Me_6TREN appears to be an efficient initiating system in a range of solvents, the catalyst deactivation is significant during the polymerization of acrylamides in EtOH and *n*-PrOH.

In contrast, the higher branched alcohols *i*-PrOH and *t*-BuOH gave conversions of over 75% for target DPs of 50, 100, and 200 (Table 1). First-order kinetic plots (Figures 3A and 4A) show noticeable curvature, especially in the early stage of polymerization; however, the PDI remains narrow, and polymer MW increases linearly with conversion (Figures 3B and 4B), indicating again that the curvature is due to progressive catalyst deactivation rather than chain termination.[43] The catalyst deactivation is significantly diminished in these branched alcohols, although still not eliminated. Polymerizations in *t*-BuOH became extremely viscous at high conversions, making sampling of high-MW polymers more difficult than in *i*-PrOH reactions at similar conversions.

Targeting higher molecular weights (M:I = 400) in *i*-PrOH gave lower conversions (~70%), a distinctly nonlinear kinetic plot (not shown), and a low molecular weight tail in the GPC (PDI = 1.27). Control was reestablished by increasing the initial monomer concentration from 33% to 50 wt %, which also resulted in faster polymerizations.

Importantly, molecular weights ($M_{n,GPC}$) increased linearly with conversion for all M:I values including 400, the highest studied. PDIs were low (1.1−1.2) during the polymerizations in *i*-PrOH and decreased from 2 to below 1.2 during polymerizations in *t*-BuOH (Figures 3B and 4B). The apparent M_n values measured by GPC were about twice as high as expected, as first observed by Müller's group.[25] The linearity of the $M_{n,GPC}$ vs conversion plots and the low PDIs reveals well-controlled polymerizations, with chains that remain active throughout the polymerization.

Thus, *i*-PrOH and *t*-BuOH allow the preparation of PNIPAM with good conversion, controlled MW, and low PDI. Hydrogen bonding between these branched alcohols and amide groups may alleviate, but not eliminate, catalyst deactivation.

PNIPAM Chain Extension. The living nature of the ATRP was confirmed by chain extension experiments. ATRP of NIPAM (M:I = 50:1) in *i*-PrOH was carried out for 4 h to 80% conversion, before adding another equivalent of NIPAM dissolved in *i*-PrOH such that the total M:I was 100:1. The polymerization was continued for another 6 h leading to a total conversion of 65%, corresponding to a conversion of only 50% during the chain extension, but the PDI remained low (1.15). In contrast, addition of another equivalent of catalyst with the second portion of NIPAM raised the total conversion to 78% after 6 h, corresponding to 76% for the chain extension. Figure 5 shows the GPC traces of the PNIPAM chain extension experiment with additional catalyst, indicating a molecular weight increase consistent with conversion and a narrow PDI. There is a small low MW shoulder indicating some termination takes place during the second monomer addition.

These observations support the idea that catalyst deactivation, not loss of end group, causes the apparently nonlinear kinetics.

Mass Spectrometric Analysis of Molecular Weight and Chain Ends. PNIPAM samples were prepared in *i*-PrOH or *t*-BuOH with good conversions, controlled MWs, and low PDIs. MALDI−TOF mass spectrometry was used to examine some of these poly-

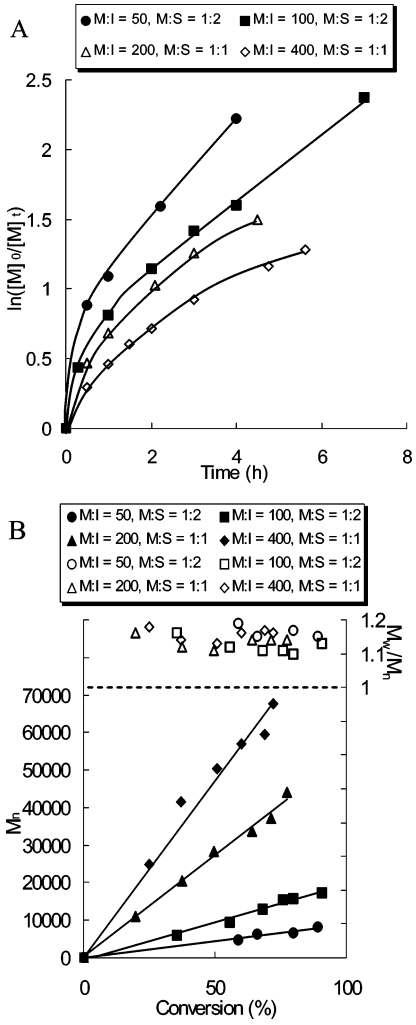

Figure 3. (A) Kinetic plot for the ATRP of NIPAM in *i*-PrOH. (B) Dependence of molecular weight ($M_{n,GPC}$) and polydispersity (M_w/M_n) on conversion. Conditions: NIPAM/*i*-PrOH = 1/2 or 1/1 (w/w); MCP:CuCl:Me_6TREN = 1:1:1; room temperature. The lines in (A) serve as guides for the eye while those in (B) are best-fit lines.

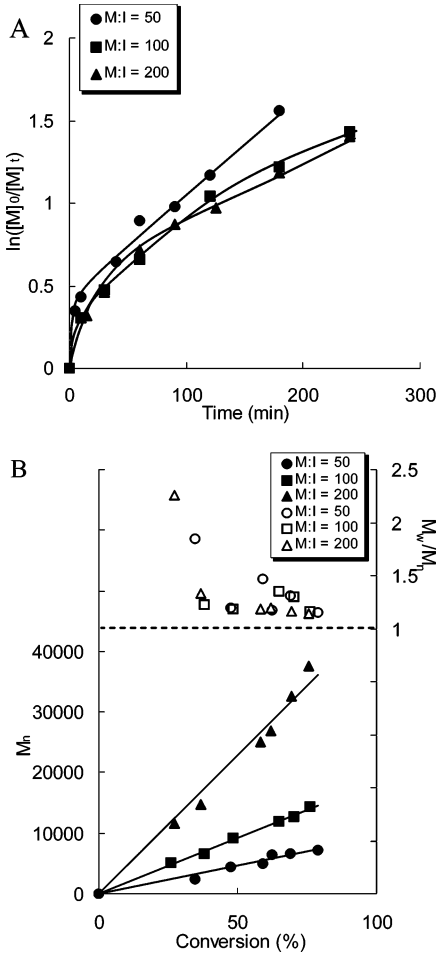

Figure 4. (A) Kinetic plot for the ATRP of NIPAM in*t*-BuOH. (B) Dependence of molecular weight ($M_{n,GPC}$) and polydispersity (M_w/M_n) on conversion. Conditions: NIPAM/*t*-BuOH = 1/2 (w/w); MCP:CuCl:Me_6TREN = 1:1:1; room temperature. The lines in (A) serve as guides for the eye while those in (B) are best-fit lines.

mers to confirm the MW and PDI and identify the end groups, in analogy with previous studies.[32,35,44−47] We focused on lower MW samples (<10 kDa) since larger samples gave weak or nonexistent signals. Similar end groups were observed for PNIPAM samples made in *i*-PrOH or *t*-BuOH, and we believe that many of the observed end groups are due to the MALDI ionization process rather than the polymerization, as discussed below.

The MALDI−TOF mass spectrum of a PNIPAM sample prepared in *t*-BuOH (M:I = 50:1, entry 10 in Table 1) is shown in Figure 6. Figure 6A shows an envelope of peaks centered at 4000 Da and extending from 1000 to 7000 Da. These MALDI data give M_n = 4000 Da, similar to that determined by NMR (4500 Da) but, as expected,[25] less than that estimated by GPC (7250 Da). The MALDI PDI value of 1.08 for this sample is lower than the 1.15 measured by GPC but confirms that the sample has a narrow MW distribution. The expanded spectrum (Figure 6B) reveals a repeating set of four peaks separated from neighboring sets by the monomer molecular weight (113 Da). The four peaks are attributed to chains bearing a methyl propionate (MePr) residue at one end and an H, ene, OH, Cl, or a lactone residue at the other end. For instance, the peak at *m/z*

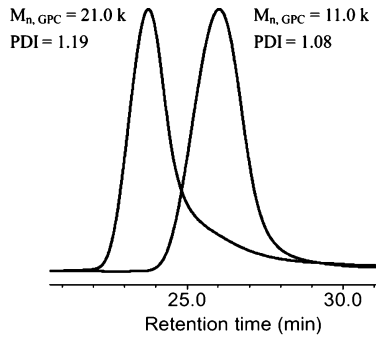

Figure 5. Gel permeation chromatograms for PNIPAM made (a) with M:I = 50:1 (80% conversion) and (b) by chain extension of the polymer with additional equivalents of both NIPAM and catalyst (total M:I = 100:1, total conversion = 78%).

= 3844.0 corresponds to MePr−$(NIPAM)_{33}$−H/Na^+ (3845.3 calcd) and/or its unsaturated analogue (3843.3 calcd). The peaks at *m/z* = 3861.6 and 3880.2 correspond to MePr−$(NIPAM)_{33}$−OH/Na^+ (3861.3 calcd) and MePr−$(NIPAM)_{33}$−Cl/Na^+ (3879.8 calcd), respectively. The final peak at *m/z* = 3802.7 was assigned to a chain of DP = 33 that had undergone a cyclization to form a lactone end group (3802.3 calcd), as shown in Scheme 2.

Figure 6C shows part of a higher resolution MALDI-quadrupole time-of-flight (QTOF) spectrum for the same

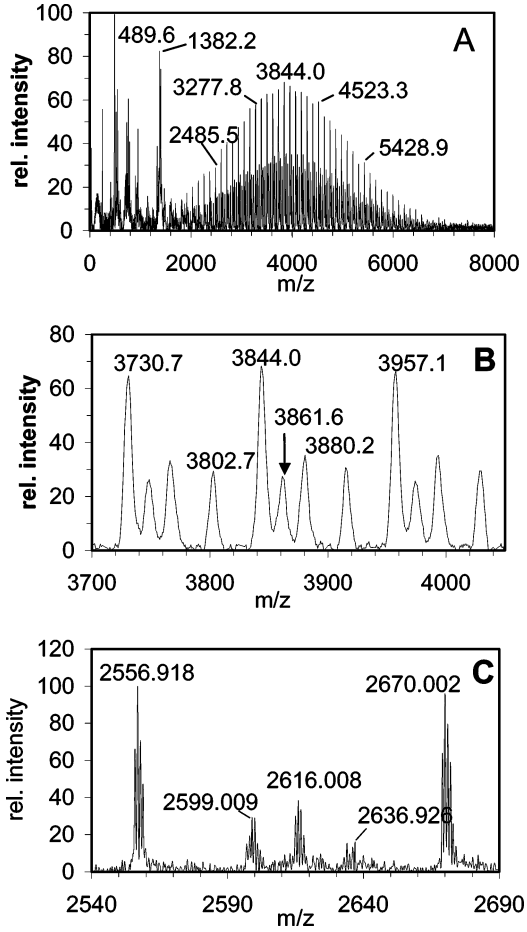

Figure 6. (A) MALDI−TOF spectra for PNIPAM sample made in *t*-BuOH (M:I = 50:1, entry 10 in Table 1). (B) expansion of spectrum A showing chains with DP = 32−34. (C) MALDI-QTOF spectrum of the same sample showing isotopic pattern for macromolecular species with DP = 22.

Scheme 2

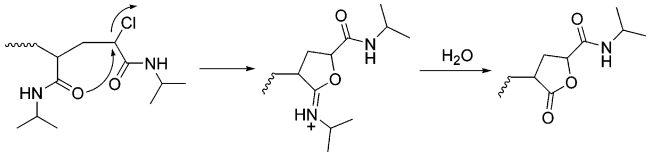

sample. The region shown is for chains with DP = 22 and the isotopic pattern for each species is clearly resolved. The major set of peaks, centered at *m/z* = 2556.9, is now due to the lactone-terminated chain rather than the H-terminated one, likely the result of a small difference in the ionization process between the two experiments. This points to the difficulties in using the apparent end group chemistry as determined by MALDI−TOF to draw conclusions about the ATRP. The set of peaks due to the H-terminated chain, beginning at 2599.0, reveals the presence of a species with *m/z* 2 mass units lower, presumably the unsaturated analogue.

While H- and ene-terminated chains may result from disproportionation during polymerization, halogen-terminated polymer chains are known to form H, OH, ene, and lactone end groups during mass spectrometric analysis,[32,44−47] and similar processes occur during MALDI−TOF analysis of dithioester-terminated PNIPAM made by RAFT.[25] In addition, termination during PNIPAM polymerization is believed to occur by coupling rather than disproportionation,[25] and peaks for

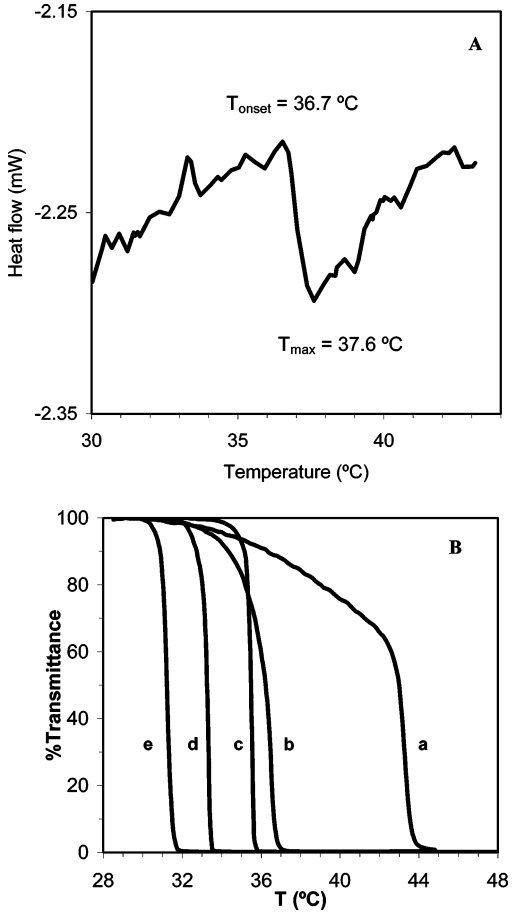

Figure 7. (A) DSC thermogram for 1 wt % solution of PNIPAM sample with $M_{n,NMR}$ = 6.5 kDa and PDI = 1.09. Heating rate = 1.0 °C/min. (B) Transmittance vs temperature for 1 wt % solutions of PNIPAM made by (a−d) ATRP or (e) conventional free-radical polymerization: $M_{n,NMR}$ = (a) 2.8, (b) 6.5, (c) 10.9, (d) 26.5, and (e) $M_{n,GPC}$ = 28.9 kDa. Heating rate = 0.2 °C/min.

the coupled product, MePr−(NIPAM)$_{33}$−MePr/Na$^+$ (3931.3 calcd), are weak or nonexistent. Lactone or related end groups are thought to occur during mass spectrometric analysis of poly(methyl methacrylate)[44,46,47] and PDMA[32] prepared by ATRP. Thus, the H, OH, ene, and lactone end groups detected for PNIPAM in this work are believed to be formed during ionization in the mass spectrometer rather than during polymerization or subsequent handling. The MALDI−TOF results are hence consistent with a PNIPAM sample composed principally of chains bearing one MePr and one chloro end group and provide further evidence that the ATRP of NIPAM was successful, producing narrow-disperse PNIPAM with well-defined end groups.

Effect of Polymer MW on Thermal Phase Transitions. DSC and turbidimetry were used to measure endotherms and cloud points, respectively, for 1 wt % aqueous solutions of the PNIPAMs prepared by ATRP. Figure 7A shows a DSC trace obtained upon heating a 1 wt % solution of PNIPAM with $M_{n,NMR}$ = 6.5 kDa and PDI = 1.09. Heating rates of 1 °C/min were used in order to obtain reasonably strong endotherms, given the small sample volumes of 30 μL chosen to minimize thermal lag.

Figure 7B shows the transmittance vs temperature plots (cloud point curves) for PNIPAM with $M_{n,NMR}$ ranging from 2.8 to 26.5 kDa obtained with a heating rate of 0.2 °C/min. Also shown in Figure 7B is the cloud

Table 2. Phase Transition Temperature of PNIPAM as a Function of Molecular Weight

			phase transition temp (°C)	
$M_{n,th}$ (kDa)	$M_{n,NMR}$ (kDa)	PDI[a]	turbidity[b] (90/50%T)	DSC[c] (onset/max)
3.3	2.8	1.07	36.3/43.0	43.3/47
5.0	5.0	1.15	37.5/38.9	39.7/41.7
7.0	6.5	1.09	34.3/36.3	36.7/37.6
8.6	6.7	1.16	36.1/36.4	36.5/38.2
13.2	10.9	1.11	35.1/35.5	35.6/36.4
17.9	15.7	1.13	34.4/34.6	34.7/35.5
32.5	26.5	1.16	32.7/33.3	33.5/34.4
d	28.9[d]	2.00	30.8/31.2	29.3/31.6

[a] Measured by GPC. [b] 1 wt % solution; heating rate = 0.2 °C/min. [c] 1 wt % solution; heating rate = 1.0 °C/min. [d] Prepared by conventional free radical polymerization. M_n measured by GPC.

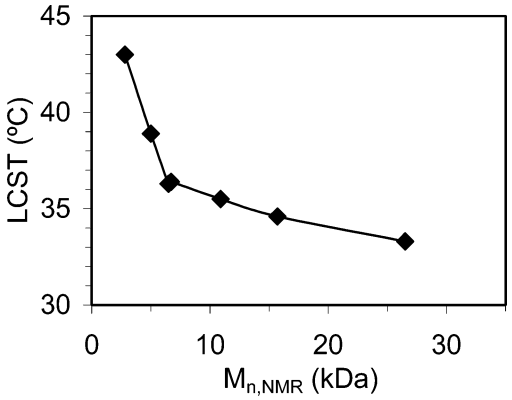

Figure 8. Cloud point (50%T) vs polymer molecular weight ($M_{n,NMR}$) for narrow-disperse PNIPAM samples made by ATRP. Cloud points determined by turbidimetry on 1 wt % solutions; heating rate = 0.2 °C/min.

point curve for a polydisperse PNIPAM sample prepared by conventional free radical polymerization ($M_{n,GPC}$ = 28.9 kDa). While the transitions are quite sharp for samples with higher MW, they broaden for the lower MW samples, and the transition for the 2.8 kDa sample (curve a in Figure 7B) occurs over a >10 °C range. We attribute the early onset and broad transition observed with the 2.8, 5.0 (not shown), and 6.5 kDa samples to the hydrophobic MePr end groups on the residual low MW fractions present in these PNIPAMs. We hence use the 50% turbidity points (50% T) to interpret the polymer MW effect on the LCST and the 90% T point to reflect contributions from the hydrophobic end groups. This is discussed in more detail below. The DSC and turbidimetry results are summarized in Table 2 and show reasonable agreement.

This is to our knowledge the first study into the effect of MW on cloud point using narrow-disperse PNIPAM. As the MW ($M_{n,NMR}$) increases from 2.8 to 26.5 kDa, the cloud point (50% T) drops from 43.0 to 33.3 °C and approaches the range of 31−32 °C commonly reported for PNIPAM (Figure 8). Interestingly, a PNIPAM sample made by conventional free radical polymerization with AIBN initiator had $M_{n,GPC}$ = 28.9 kDa (note: GPC likely overestimates M_n by a factor of 2) and PDI = 2.0 and gave a cloud point of 31.2 °C. This falls within the typical range, but is about 3 °C lower than a narrow-disperse sample of similar M_n made by ATRP. This is attributed to the significant high-MW fraction present in such polydisperse samples. This fraction will have a lower LCST and thus may mask the transition of the major, but lower MW, fraction. This illustrates the importance of using narrow-disperse polymers in studies of LCST behavior.

As mentioned earlier, previous studies of PNIPAM and other thermoresponsive polymers have found the LCST to be independent,[5,14,15] directly dependent,[8,22] or inversely dependent[6,16−21] upon MW. LCSTs are expected to decrease with increasing polymer MW on the basis of the changes in the polymer−solvent interaction.[16,48] However, end groups derived from initiators, terminators, or chain-transfer agents can mitigate this trend, especially at lower MWs, by changing the hydrophobic/hydrophilic nature of the polymer. It was found that LCSTs were decreased by hydrophobic end groups and increased by hydrophilic end groups, with the magnitude of the effect depending on the nature of the end group.[14,22,49,50]

Thus, the MW effect on LCST should be seen as a combination of changes in polymer−solvent interaction, along with changes in the importance of end group contributions to the hydrophobic/hydrophilic balance of the polymer. The improved control over end groups possible with ATRP should make it possible to begin to resolve these two effects.

The PNIPAM studied in this work bears MePr and chloro end groups. Methyl propionate itself is weakly hydrophobic (6.4 wt % solubility in water at 20 °C)[51] and does not appear to have a significant effect on the cloud points of the higher MW polymers studied here. However, in oligomeric PNIPAM, the MePr end group could perturb the hydrophobic/hydrophilic balance enough to show a lower onset of the cloud point, seen most clearly in the 90%T data. In fact, we attribute the early onset and low-temperature slopes observed in the turbidity curves of the 2.8, 5.0, and 6.5 kDa samples (see Figure 7B) to the MePr end group. These low MW samples will possess significant oligomeric fractions less than 1 kDa, which would be sensitive to the hydrophobic effect of the MePr end group and show early phase separation seen in 90% T. We plan to test this hypothesis by preparing oligomeric PNIPAM samples bearing MePr end groups. Given the low hydrophobicity of the MePr end group we believe this to be a minor effect that would not distort MW influence on the cloud point seen in the 50% T data.

Studies aimed at further probing the effect of a range of different end groups on the cloud points of PNIPAMs of different MWs are underway and will be reported in the near future.

Conclusion

We have shown that ATRP of NIPAM in *i*-PrOH and *t*-BuOH leads to narrow-disperse PNIPAM with high conversion and good molecular weight control. These branched alcohols are thought to hydrogen-bond to monomer and polymer, thereby reducing the known deactivation of the ATRP catalyst by acrylamides and their polymers.

Aqueous solutions of these PNIPAMs showed a dramatic decrease in cloud point with increasing MW, attributed to the reduced entropy of mixing with increasing MW.

In addition, the lowest MW samples showed an early onset of phase separation, which is attributed to the presence of oligomer that is influenced more strongly by the slightly hydrophobic MePr end group.

Hence, the use of ATRP to prepare PNIPAMs allows good control over both polymer MW and end group, an

ability that is being exploited in our current work to prepare PNIPAMs with a range of end groups of different polarity in order to study their effects on the LCST.

Acknowledgment. We thank Gina Dimopoulos-Italiano and Dr. Kirk Green for their assistance with the MALDI−TOF analysis and Dr. Paul Berti for the use of the UV−vis spectrophotometer. We acknowledge the Natural Sciences and Engineering Research Council of Canada and 3M Canada Inc. for supporting this research. Y. Xia thanks McMaster University for a James A. Morrison Memorial Scholarship.

References and Notes

(1) Heskins, M.; Guillet, J. E. *J. Macromol. Sci., Chem.* **1968**, *A2*, 1441−1455.
(2) Schild, H. G. *Prog. Polym. Sci.* **1992**, *17*, 163−249.
(3) Chen, G.; Hoffman, A. S. *Nature (London)* **1995**, *373*, 49−52.
(4) Hay, D. N. T.; Rickert, P. G.; Seifert, S.; Firestone, M. A. *J. Am. Chem. Soc.* **2004**, *126*, 2290−2291.
(5) Fujishige, S.; Kubota, K.; Ando, I. *J. Phys. Chem.* **1989**, *93*, 3311−3313.
(6) Schild, H. G.; Tirrell, D. A. *J. Phys. Chem.* **1990**, *94*, 4352−4356.
(7) Cho, E. C.; Lee, J.; Cho, K. *Macromolecules* **2003**, *36*, 9929−9934.
(8) Tong, Z.; Zeng, F.; Zheng, X. *Macromolecules* **1999**, *32*, 4488−4490. Zheng, X.; Tong, Z.; Xie, X.; Zeng, F. *Polym. J.* **1998**, *30*, 284−288.
(9) Winnik, F. M.; Ringsdorf, H.; Venzmer, J. *Macromolecules* **1990**, *23*, 2415−2416.
(10) Schild, H. G.; Muthukumar, M.; Tirrell, D. A. *Macromolecules* **1991**, *24*, 948−952.
(11) Otake, K.; Karaki, R.; Ebina, T.; Yokoyama, C.; Takahashi, S. *Macromolecules* **1993**, *26*, 2194−2197.
(12) Schild, H. G.; Tirrell, D. A. *Langmuir* **1991**, *7*, 665−671.
(13) Lee, L. T.; Cabane, B. *Macromolecules* **1997**, *30*, 6559−6566.
(14) Otake, K.; Inomata, H.; Konno, M.; Saito, S. *Macromolecules* **1990**, *23*, 283−289.
(15) Tiktopulo, E. I.; Uversky, V. N.; Lushchik, V. B.; Klenin, S. I.; Bychkova, V. E.; Ptitsyn, O. B. *Macromolecules* **1995**, *28*, 7519−7524.
(16) Lessard, D. G.; Ousalem, M.; Zhu, X. X. *Can. J. Chem.* **2001**, *79*, 1870−1874.
(17) Xue, W.; Huglin, M. B.; Jones, T. G. J. *Macromol. Chem. Phys.* **2003**, *204*, 1956−1965.
(18) Kunugi, S.; Tada, T.; Tanaka, N.; Yamamoto, K.; Akashi, M. *Polym. J.* **2002**, *34*, 383−388.
(19) Aoshima, S.; Oda, H.; Kobayashi, E *J. Polym. Sci., Part A: Polym. Chem.* **1992**, *30*, 2407−2413.
(20) Laukkanen, A.; Valtola, L.; Winnik, F. M.; Tenhu, H. *Macromolecules* **2004**, *37*, 2268−2274.
(21) Bütün, V.; Armes, S. P.; Billingham, N. C. *Polymer* **2001**, *42*, 5993−6008.
(22) Liu, Q.; Yu, Z.; Ni, P. *Colloid Polym. Sci.* **2004**, *282*, 387−393.
(23) Chiefari, J.; Chong, Y. K.; Ercole, F.; Kristina, J.; Jeffery, J.; Le, T. P. T.; Mayadunne, R. T. A.; Meijs, G. F.; Moad, C. L.; Moad, G.; Rizzardo, E.; Thang, S. H. *Macromolecules* **1998**, *31*, 5559−5562.
(24) Ganachaud, F.; Monteiro, M. J.; Gilber, R. G.; Dourges, M.; Thang, S. H.; Rizzardo, E. *Macromolecules* **2000**, *33*, 6738−6745.
(25) Schilli, C.; Lanzendörfer, M. G.; Müller, A. H. E. *Macromolecules* **2002**, *35*, 6819−6827.
(26) Ray, B.; Isobe, Y.; Matsumoto, K.; Habaue, S.; Okamoto, Y.; Kamigaito, M.; Sawamoto, M. *Macromolecules* **2004**, *37*, 1702−1710.
(27) Convertine, A. J.; Ayres, N.; Scales, C. W.; Lowe, A. B.; McCormick, C. L. *Biomacromolecules* **2004**, *5*, 1177−1180.
(28) Hawker, C. J.; Bosman, A. W.; Harth, E. *Chem. Rev.* **2001**, *101*, 3661−3688.
(29) Bosman, A. W.; Vestberg, R.; Heumann, A.; Fréchet, J. M. J.; Hawker, C. J. *J. Am. Chem. Soc.* **2003**, *125*, 715−728.
(30) (a) Matyjaszewski, K.; Xia, J. *Chem. Rev.* **2001**, *101*, 2921−2990. (b) Kamigaito, M.; Ando, T.; Sawamoto, M. *Chem. Rev.* **2001**, *101*, 3689−3746.
(31) Teodorescu, M.; Matyjaszewski, K. *Macromolecules* **1999**, *32*, 4826−4831.
(32) Rademacher, J. T.; Baum, M.; Pallack, M. E.; Brittain, W. J.; Simonsick, W. J. *Macromolecules* **2000**, *33*, 284−288.
(33) Teodorescu, M.; Matyjaszewski, K. *Macromol. Rapid Commun.* **2000**, *21*, 190−194.
(34) Neugebauer, D.; Matyjaszewski, K. *Macromolecules* **2003**, *36*, 2598−2603.
(35) Masci, G.; Giacomelli, L.; Crescenzi, V. *Macromol. Rapid Commun.* **2004**, *25*, 559−564.
(36) Jones, J. A.; Novo, N.; Flagler, K.; Pagnucco, C. D.; Carew, S.; Cheong, C.; Kong, X. Z.; Burke, N. A. D.; Stöver, H. D. H. Macromolecules, submitted; Jones, J. A. M. Sc. Thesis, McMaster University, 1999.
(37) Yin, X.; Stöver, H. D. H. *Macromolecules* **2002**, *35*, 10178−10181.
(38) Yin, X.; Stöver, H. D. H. *Macromolecules* **2003**, *36*, 9817−9822.
(39) Yin, X.; Stöver, H. D. H. *J. Polym. Sci., Part A: Polym. Chem.* **2005**, *43*, 1641−1648.
(40) Yin, X.; Stöver, H. D. H. *Macromolecules* **2005**, *38*, 2109−2115.
(41) Ciampolini, M.; Nardi, N. *Inorg. Chem.* **1966**, *5*, 41−44.
(42) Xia, J.; Zhang, X.; Matyjaszewski, K. *Macromolecules* **1999**, *32*, 3531−3533.
(43) Several polymerizations were conducted in *i*-PrOH at M:I = 50:1, with 5, 10, or 20% of the Cu(I) replaced by Cu(II). The rate of polymerization decreased steadily as 5, 10, and 20% Cu(II) was added; however, there was no change in the apparent intercept.
(44) Barner-Kowollik, C.; Davis, T. P.; Stenzel, M. H. *Polymer* **2004**, *45*, 7791−7805.
(45) Nonaka, H.; Ouchi, M.; Kamigaito, M.; Sawamoto, M. *Macromolecules* **2001**, *34*, 2083−2088.
(46) Singha, N. K.; Rimmer, S.; Klumperman, B. *Eur. Polym. J.* **2004**, *40*, 159−163.
(47) Borman, C. D.; Jackson, A. T.; Bunn, A.; Cutter, A. L.; Irvine, D. J. *Polymer* **2000**, *41*, 6015−6020.
(48) Patterson, D. *Macromolecules* **1969**, *2*, 672−677.
(49) Chung, J. E.; Yokoyama, M.; Aoyagi, T.; Sakurai, Y.; Okano, T. *J. Controlled Release* **1998**, *53*, 119−130.
(50) Chung, J. E.; Yokoyama, M.; Suzuki, K.; Aoyagi, T.; Sakurai, Y.; Okano, T. *Colloids Surf. B: Biointerfaces* **1997**, *9*, 37−48.
(51) *Solubility Data Series*; Getzen, F., Hefter, G., Maczynski, A., Eds.; Pergamon: Oxford, 1992; Vol. 48, pp 138−147.

MA050261Z